

The Niemann-Pick C1 Inhibitor NP3.47 Enhances Gene Silencing Potency of Lipid Nanoparticles Containing siRNA

Haitang Wang¹, Yuen Yi C Tam¹, Sam Chen¹, Josh Zaifman^{1,2}, Roy van der Meel^{1,3}, Marco A Ciufolini² and Pieter R Cullis¹

¹Department of Biochemistry and Molecular Biology, University of British Columbia, Health Sciences Mall, Vancouver, British Columbia, Canada;

²Department of Chemistry, University of British Columbia, Vancouver, British Columbia, Canada; ³Department of Clinical Chemistry and Hematology, University Medical Center Utrecht, Heidelberglaan, Utrecht, The Netherlands

The therapeutic applications of lipid nanoparticle (LNP) formulations of small interfering RNA (siRNA), are hampered by inefficient delivery of encapsulated siRNA to the cytoplasm following endocytosis. Recent work has shown that up to 70% of endocytosed LNP-siRNA particles are recycled to the extracellular medium and thus cannot contribute to gene silencing. Niemann-Pick type C1 (NPC1) is a late endosomal/lysosomal membrane protein required for efficient extracellular recycling of endosomal contents. Here we assess the influence of NP3.47, a putative small molecule inhibitor of NPC1, on the gene silencing potency of LNP-siRNA systems *in vitro*. Intracellular uptake and colocalization studies revealed that the presence of NP3.47 caused threefold or higher increases in accumulation of LNP-siRNA in late endosomes/lysosomes as compared with controls in a variety of cell lines. The gene silencing potency of LNP siRNA was enhanced up to fourfold in the presence of NP3.47. Mechanisms of action studies are consistent with the proposal that NP3.47 acts to inhibit NPC1. Our findings suggest that the pharmacological inhibition of NPC1 is an attractive strategy to enhance the therapeutic efficacy of LNP-siRNA by trapping LNP-siRNA in late endosomes, thereby increasing opportunities for endosomal escape.

Received 29 January 2016; accepted 10 August 2016; advance online publication 1 November 2016. doi:10.1038/mt.2016.179

INTRODUCTION

The application of RNA interference using small interfering RNA (siRNA) has enormous therapeutic potential, as virtually every gene becomes a “druggable” target that can be selectively silenced. However, in the free form, the large, negatively charged siRNA molecules are subject to degradation by RNases in the circulation, are rapidly cleared from the blood and cannot penetrate cell membranes to access intracellular sites of action even if they get to target tissues.¹ Considerable effort has therefore been made to develop safe and efficient delivery systems. Lipid nanoparticles (LNPs) are the most advanced delivery systems with several LNP

siRNA formulations undergoing clinical evaluation.² These systems employ optimized ionizable cationic lipids and satisfy key issues for the development of clinically relevant siRNA-loaded LNP (LNP-siRNA) including efficient siRNA encapsulation, high gene silencing potencies and therapeutic indices (for liver targets) as well as scalable manufacturing processes.^{3–5} However, there remains a critical need to improve the potency of LNP-siRNA systems in order to extend applications of this gene silencing technology to tissues other than the liver.

A critical determinant of gene silencing potency involves the cellular processing of LNP-siRNA following endocytosis. A recent study suggests that < 2% of endocytosed LNP-siRNA is actually released into the cytoplasm,⁶ and other studies have demonstrated that the majority of internalized LNP-siRNA is recycled back to the extracellular environment.⁷ Niemann-Pick type C-1 protein (NPC1) has been identified as an important regulator of major recycling pathways of siRNA delivered by LNPs; NPC1 knockout cells showed enhanced siRNA intracellular retention and increased gene silencing.⁷ NPC1 is a late endosomal/lysosomal membrane protein that mediates cellular cholesterol trafficking; loss of NPC1 function has been shown to cause a hyper-accumulation of cholesterol in lysosomes, resulting in Niemann-Pick disease type C.⁸ This work therefore suggests that the pharmacological inhibition of NPC1 could be an attractive strategy to potentiate therapeutic effects of LNP-siRNA by reducing recycling to the extracellular milieu, increasing intracellular retention and thus maximizing the potential for endosomal release of siRNA into the cell cytoplasm.

In a screen of small molecules to identify agents that prevent Ebola virus infection, the compound NP3.47 (Figure 1) was shown to enhance cholesterol accumulation in intracellular vacuoles,⁹ presumably by preventing endosomal escape of lipoproteins following endocytosis. In the case of Ebola virus it was shown that NP3.47 inhibited NPC1 and blocked cytoplasmic delivery of the virus.⁹ For LNP-siRNA systems, longer residence times in intracellular organelles may be expected to result in an enhanced possibility for lytic interactions of component cationic lipids with late endosome or lysosome membranes, resulting in siRNA escape into the cytosol. To assess the influence of NP3.47 on the processing of LNP-siRNA following uptake, various cell lines were incubated with LNP-siRNA in the presence and absence of NP3.47

Correspondence: Pieter Cullis, Department of Biochemistry and Molecular Biology, University of British Columbia, 2350 Health Sciences Mall, Vancouver, British Columbia V6T 1Z3, Canada. E-mail: pieterc@mail.ubc.ca

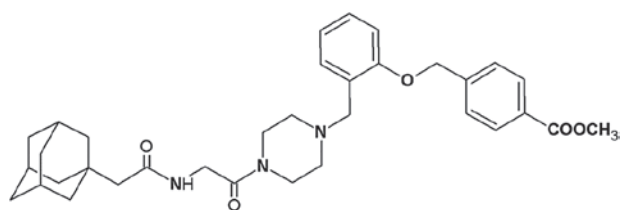


Figure 1 Chemical structure of NP3.47. Reprinted from ref. 9

to determine effects on intracellular accumulation, extracellular recycling, and gene silencing. It is shown that the presence of NP3.47 increases intracellular accumulation, delays recycling to the cell exterior and enhances the gene silencing potency of LNP-siRNA systems, indicating that NPC1 inhibition is a rational strategy for improving the potency of LNP-siRNA systems.

RESULTS

The presence of NP3.47 increases intracellular localization of LNP-siRNA

The NPC1 protein plays an important role in the intracellular trafficking of cholesterol, as indicated by the fact that NPC1 knockout cells demonstrate high levels of cholesterol.⁷ In order to show that NP3.47 (which was identified as a blocker of Ebola infection) has effects consistent with inhibition of NPC1 the effects of NP3.47 on cholesterol accumulation in HeLa cells was examined. As shown in **Supplementary Figure S1**, the presence of NP3.47 resulted in significantly higher levels of intracellular cholesterol. The compound U 18666A, which is known to increase intracellular cholesterol by inhibiting cholesterol transport from lysosomes¹⁰ was used as a positive control. It may be noted that the presence of U 18666A reduces LNP uptake in contrast to the increased accumulation of LNP in NPC knockout cells.⁷

Next, we investigated the effects of NP3.47 on LNP accumulation in a variety of cell lines. LNP siRNA systems containing the ionizable cationic lipid MC3 were formulated using the microfluidic mixing technique¹¹ and administered to cells in the presence and absence of NP3.47. The cell lines employed were NIH/3T3, HeLa, LNCaP, Raw 264.7, OVCAR-3, PC3, 22Rv1, and NPC1 knockout (NPC1^{-/-}) cells which were incubated with DiI-labeled LNP-siRNA and NP3.47 at 0, 1 or 10 μmol/l for 24 hours. Intracellular accumulation of LNP-siRNA was determined by quantification of DiI fluorescence using the Cellomics Arrayscan. Results are shown in **Figure 2**, where it may be noted that, in the absence of NP3.47, accumulation as reflected by fluorescence intensity increased up to a dose level of 2.5 mg/l but was reduced at the highest dose of 5 mg/l. Similar effects have been observed elsewhere for related LNP systems and arise due to inhibitory effects of the high concentrations of the exchangeable PEG-lipid¹² at higher LNP dose levels (Kulkarni *et al.*, unpublished results).

The results shown in **Figure 2a–h** demonstrate that in the presence of 10 μmol/l NP3.47, LNP-siRNA (2.5 and 5 mg/l concentrations) accumulated significantly more in all cell lines tested compared with untreated cells. This is with the exception of NPC1^{-/-} cells where NP3.47 had no effect. Representative images (**Figure 2i**) illustrate the increased intracellular LNP accumulation in the presence of 10 μmol/l NP3.47. All subsequent experiments were carried out using 10 μmol/l concentrations of NP3.47.

NP3.47 decreases and delays LNP-siRNA recycling to the cell exterior

The absence of NPC1 has been shown to reduce the extracellular recycling of siRNA delivered by LNPs.⁷ To determine the effect of the NPC1 inhibitor NP3.47 on siRNA recycling, HeLa cells were incubated with fluorescently-labeled siRNA encapsulated in LNPs in the presence and absence of the inhibitor. The Quasar 570-tagged siRNA was selected because previous work shows that the distribution pattern of Quasar 570 reflects the intact siRNA localization.¹³ The cellular recycling of LNP-siRNA was determined by measuring the intracellular and extracellular amount of siRNA over time using the pulse-chase protocol outlined in the “Methods” section. As shown in **Figure 3**, in the absence of NP3.47, ~60% of the previously internalized siRNA was detected in the supernatant 4 hours after noninternalized LNP-siRNA was removed. The presence of NP3.47 reduced siRNA exocytosis, as only 40% of the previously internalized siRNA was detected extracellularly 4 hours after external LNP siRNA was removed. It is interesting to note however, that the bulk of the internalized siRNA is eventually recycled to the cell exterior. After a 24 hours chase, 80% of the total internalized siRNA was detected in the extracellular medium in the absence of NP3.47, as compared with ~70% of the siRNA when the NPC1-inhibitor was present. These results indicate that the presence of NP3.47 reduces and delays siRNA recycling to the extracellular milieu.

The presence of NP3.47 enhances the gene silencing potency of LNP-siRNA

To determine if the increased intracellular cellular accumulation of LNP-siRNA induced by NP3.47 could lead to enhanced gene silencing, HeLa OVCAR-3, PC3, 22Rv1 or NPC1^{-/-} cells were treated for 24 hours with LNPs containing small interfering glycerolaldehyde 3-phosphate dehydrogenase (siGAPDH) (LNP-siGAPDH) in the absence or presence of 10 μmol/l NP3.47. Quantification of GAPDH mRNA levels by reverse transcription-quantitative polymerase chain reaction (RT-qPCR) indicated dose-dependent gene silencing induced by increasing concentrations of LNP-siGAPDH. In order to ascertain the effects of NP3.47 the siRNA dose required to induce 50% gene silencing (ED₅₀) was determined. Gene silencing was enhanced approximately fourfold in HeLa cells (ED₅₀ 0.06 versus 0.24 mg/l) and approximately twofold in OVCAR-3 (ED₅₀ 0.13 versus 0.28 mg/l), PC3 (ED₅₀ 0.16 versus 0.28 mg/l), and 22Rv1 cells (ED₅₀ 0.025 versus 0.065 mg/l) in the presence of 10 μmol/l NP3.47 (**Figure 4a–d**). Although the gene silencing enhancement by NP3.47 is less than that reported by Sahay *et al.*,⁷ for NPC1 knockout cells, the results support the hypothesis that NP3.47 inhibits recycling mediated by NPC1 resulting in enhanced siRNA escape into the cytosol. For NPC1^{-/-} cells, there was no change in (ED₅₀) observed between the NP3.47 treated and LNP-siRNA alone (**Figure 4e**), again consistent with hypothesis.

NP3.47 does not influence acidification of intracellular organelles

If NP3.47 is enhancing intracellular accumulation of LNP-siRNA systems, by inhibiting the action of the NPC1 protein, it would not be expected to affect acidification of endosomes as they progress

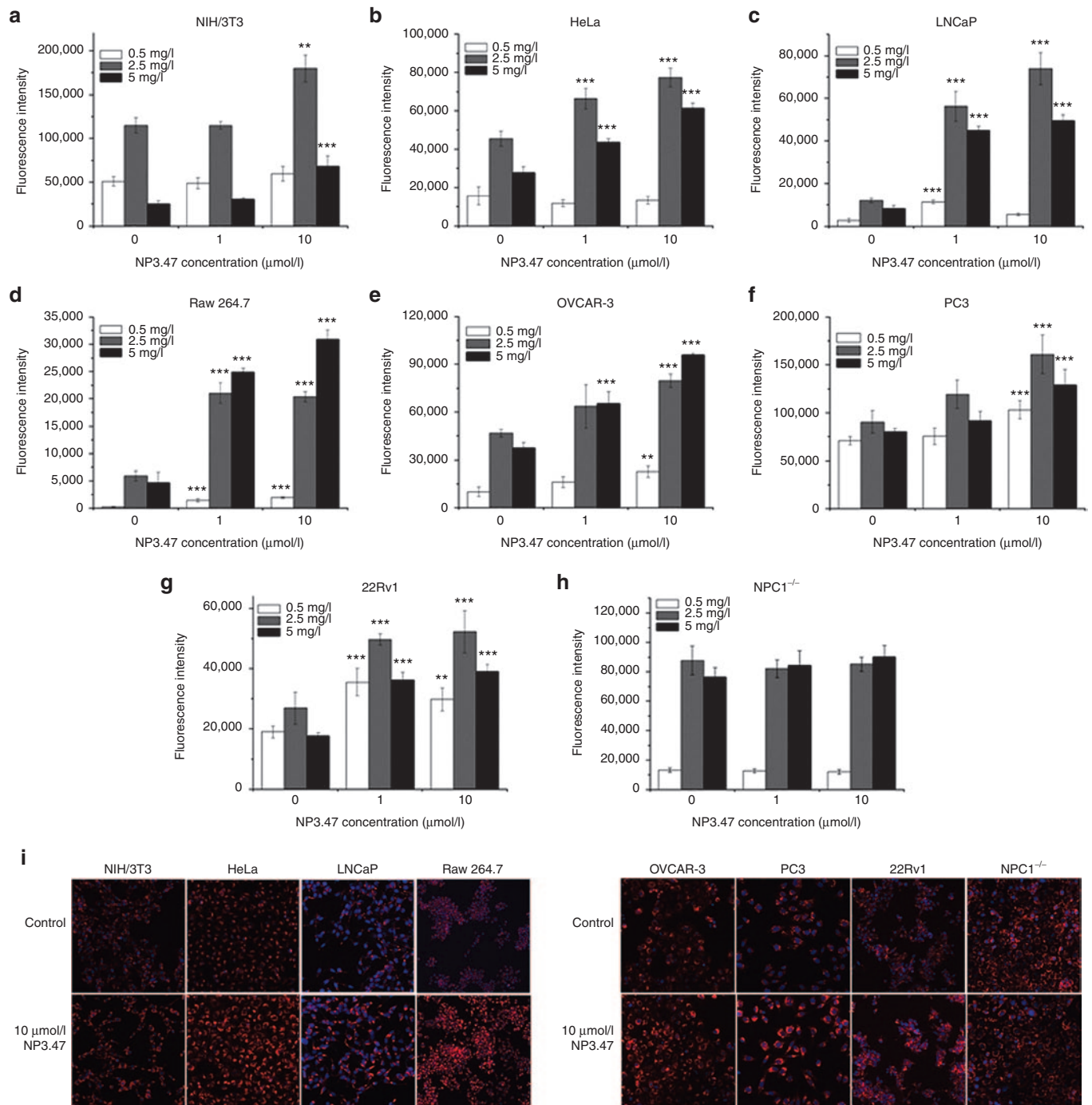


Figure 2 The intracellular accumulation of LNP-siRNA is increased in the presence of NP3.47. **(a)** NIH/3T3, **(b)** HeLa, **(c)** LNCaP, **(d)** Raw 264.7, **(e)** OVCAR-3, **(f)** PC3, **(g)** 22Rv1, and **(h)** NPC1^{-/-} cells were exposed to Dil-labeled LNP-siRNA (0.5, 2.5, and 5 mg/l) and NP3.47 (0, 1, and 10 μmol/l) for 24 hours at 37°C. Accumulation of LNP-siRNA was monitored using a Celloomics Arrayscan and quantified using the Celloomics Compartmental Analysis algorithm. Data are presented as mean ± SD of three representative experiment performed in triplicate (***P* < 0.01, ****P* < 0.001 versus controls, by unpaired Student's *t*-test). **(i)** Representative images of cells exposed to LNP-siRNA (2.5 mg/l) with and without treatment of 10 μmol/l NP3.47. LNP-siRNA, siRNA-loaded LNP; LNP, lipid nanoparticle; siRNA, small interfering RNA; SD, standard deviation.

toward lysosomes. Live cell imaging was used to determine the effects of NP3.47 on the acidification of endosomal/lysosomal compartments (**Figure 5**). Lysosomotropic dyes (LysoTracker Green or Lysoview 633) possess weakly basic amine groups which selectively accumulate in low intracellular pH compartments and have been used to label and track acidic organelles in live

cells.¹⁴ Increases of the pH in previously acidic organelles can be visualized as a reduction of fluorescence intensity and/or a loss in the ability to visualize intracellular structures by fluorescence microscopy. Ammonium chloride, a lysosomal inhibitor that acts by increasing lysosomal pH,¹⁵ was used as a positive control. The compound 4-bromobenzaldehyde *N*-(2,6-dimethylphenyl)

semicarbazone (EGA), reported to delay lysosomal maturation without neutralizing acidic organelles,¹⁶ was used as a negative control.

As shown in **Figure 5**, live cell imaging using confocal microscopy demonstrated that ammonium chloride significantly reduced the intracellular fluorescence intensity of the lysosomotropic agents (LysoTracker Green and LysoView 633) when incubated with Raw 264.7, NIH/3T3 and HeLa cells. However, the presence of NP3.47 at either 1 $\mu\text{mol/l}$ or 10 $\mu\text{mol/l}$ concentrations did not reduce fluorescence intensities of intracellular structures in any of the cell lines, indicating that the small molecule inhibitor does not neutralize acidic organelles involved in endocytic pathways. This behavior was similar to that observed for EGA and indicates that the mechanism behind the increased intracellular accumulation of LNP-siRNA and enhanced gene silencing in the presence of NP3.47 does not result from neutralizing previously acidic endocytic compartments.

NP3.47 enhances delivery of internalized LNP-siRNA to late endosomes and lysosomes

If NP3.47 delays and reduces recycling of siRNA to the exterior of the cell and does not affect the acidification of endocytotic organelles, it would be expected that increased trafficking of LNP systems to late endosomes and lysosomes should be observed. Pulse-chase colocalization studies of LNP-siRNA with endosomal/lysosomal markers in HeLa cells were therefore performed in the presence and absence of NP3.47 and then visualized by confocal microscopy. HeLa cells were incubated with DiI-labeled LNP-siRNA for 3 hours after which the cells were washed and resuspended in fresh medium. Cells were fixed after 15 minutes or 60 minutes chase and endosomes/lysosomes were visualized by staining with anti-early endosomal antigen-1 (EEA1) and anti-lysosomal associated membrane protein-1 (LAMP1) antibodies, respectively as shown in **Figure 6**.

Confocal imaging demonstrated little colocalization of LNP-siRNA with EEA1 after 15 and 60 minutes chase, regardless of whether NP3.47 was present or not. However, distinct colocalization of LNP-siRNA with LAMP1 was observed after 15 and 60 minutes chase. Interestingly, quantification of the confocal images revealed that colocalization of LNP-siRNA with LAMP1 at both time points was significantly enhanced in the presence of NP3.47 (**Figure 6c,d**). An increase in localization of LNPs with LysoView-positive vesicles (late endosome and lysosome markers) was also observed in live cells (3 hours pulse and 60-minutes chase, **Supplementary Figure S2**) treated with NP3.47. These results indicate that the enhanced knockdown of LNP-siRNA in the presence of NP3.47 is mediated by enhanced trapping of LNP in late endosomal/lysosomal compartments, which is in agreement with previous findings in NPC1^{-/-} cells.⁷

DISCUSSION

The results of this work show that the presence of the NPC1 inhibitor NP3.47 can enhance intracellular accumulation of LNP-siRNA systems *in vitro*, resulting in up to fourfold increases in gene silencing potency. There are three aspects of these results that require discussion. The first concerns the mechanism whereby NP3.47 exerts its effects and whether the results presented are

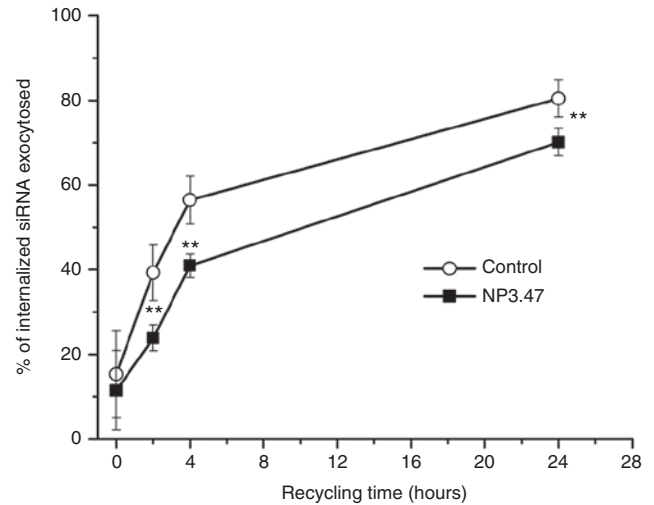


Figure 3 Cellular recycling of siRNA is delayed by NP3.47. HeLa cells were treated for 3 hours with Quasar 570 labeled LNP-siRNA in the presence or absence of 10 $\mu\text{mol/l}$ NP3.47. Cells were washed to remove extracellular LNP-siRNA and fresh medium was added containing 10 $\mu\text{mol/l}$ NP3.47 or DMSO as a control. At different time points, the supernatant and cell lysate were collected to quantify the fluorescent siRNA. The ratio of extracellular siRNA concentration to total concentration is plotted. Data are presented as mean \pm SD of three representative experiments performed in triplicate (** $P < 0.01$ versus control by unpaired Student's *t*-test). DMSO, dimethylsulfoxide; LNP-siRNA, siRNA-loaded LNP; LNP, lipid nanoparticle; siRNA, small interfering RNA.

fully consistent with inhibition of the function of NPC1. Second, the results presented here indicate that the presence of NP3.47 enhances accumulation in lysosomes; this may not be expected to result in enhanced gene silencing due to potential degradation of LNP-siRNA contents. The third area of discussion concerns how the benefits of agents such as NP3.47 could be extended to *in vivo* applications. We discuss these areas in turn.

With regard to the mechanism of action of NP3.47, a number of the results reported here support the proposal that NP3.47 acts through inhibition of NPC1. First, results indicate that the enhanced intracellular accumulation of LNP-siRNA is due to a delay and reduction in the amount of siRNA that is recycled to the cell exterior in the presence of NP3.47. This is consistent with inhibition of the NPC1 protein as NPC1 has been shown to be required for extracellular recycling of endosomal contents.⁷ Second, we demonstrate that NP3.47 does not neutralize acidic intracellular organelles. Such neutralization would inhibit progression to late endosomes and lysosomes;¹⁷ thus the lack of influence of NP3.47 on the intracellular organelle pH is also consistent with the significantly higher levels of LNP-siRNA that are observed to accumulate in late endosomes and lysosomes in the presence of NP3.47. Third, in addition to extracellular recycling, NPC1 has also been shown to be necessary for the efficient fusion of lysosomes with late endosomes.¹⁸ Continuous fusion of lysosomes with late endosomes creates hybrid organelles in which the bulk of the lysosomal cargo is degraded.^{18,19} NPC1 dysfunction caused accumulation of lysosomal cargo,¹⁸ again consistent with the results presented here which show that more LNP colocalize with late endosomes/lysosomes in the presence of NP3.47.

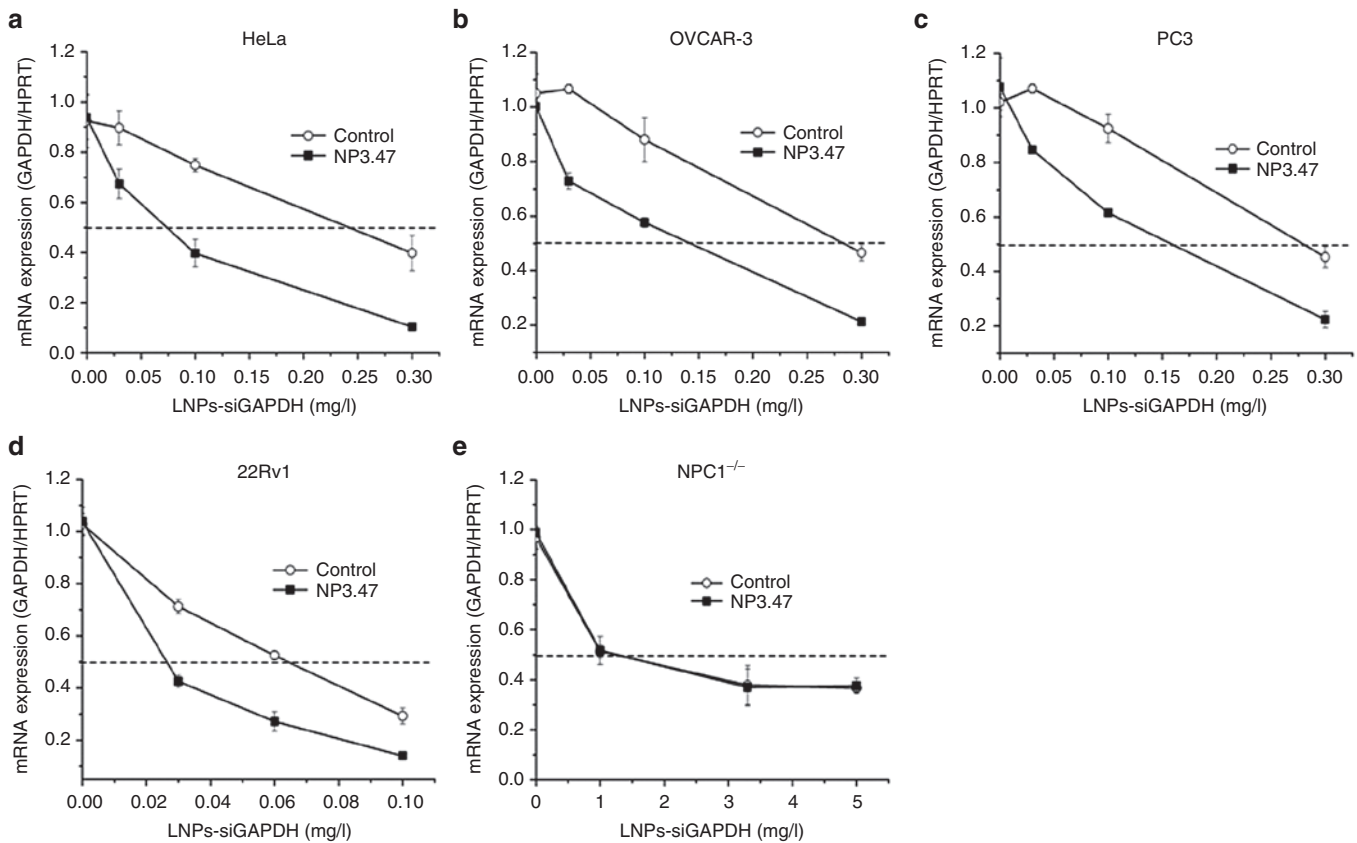


Figure 4 NP3.47 enhances the potency of LNP-siRNA formulations for gene silencing *in vitro*. (a) HeLa, (b) OVCAR-3, (c) PC3, (d) 22Rv1, and (e) NPC1^{-/-} cells were treated with LNPs-siRNA against GAPDH in the presence or absence of 10 μ mol/l NP3.47. GAPDH mRNA levels were quantified after 24 hours incubation using RT-qPCR. A median effective siRNA dose (ED50) for the control and the NP3.47 treated can be obtained. Data are presented as mean \pm SD of three representative experiments performed in triplicate. GAPDH, glyceraldehyde 3-phosphate dehydrogenase; LNP-siRNA, siRNA-loaded LNP; LNP, lipid nanoparticle; RT-qPCR, reverse transcription quantitative polymerase chain reaction; siRNA, small interfering RNA.

An additional question concerning the mechanism of NP3.47 is whether it applies to other forms of endocytosis. The endocytosis of LNP-siRNA systems containing ionizable cationic lipids is dependent on association with apolipoprotein E (ApoE) and proceeds by the classic clathrin-mediated endocytosis mechanism used for uptake of cholesterol-containing LDL.²⁰ However, it has been noted that low NPC1 levels result in reduced internalization and lower transfection efficiencies for a polymer-based gene delivery system which enters cells primarily through caveolae-mediated endocytosis.²¹ Thus, the benefits of NP3.47 on LNP-siRNA intracellular accumulation and gene silencing potencies may depend on the particular endocytotic mechanism employed.

The observation that the presence of NP3.47 leads to enhanced lysosomal accumulation of LNP-siRNA systems and enhanced gene silencing capabilities is interesting for a number of reasons. First, it has not been generally recognized that such a large proportion of endocytosed siRNA is recycled to the extracellular medium (>60% for HeLa cells). Such recycling could be a factor limiting the gene silencing potency of LNP-siRNA systems following uptake contributing to the fact that only a minor fraction (<-2%⁶ and ~3.5%²²) of endocytosed siRNA is released into the cytosol. Second, the fact that greater accumulation of LNP-siRNA systems is observed in lysosomes in the presence of NP3.47 implies that they have passed through late endosomes and

thus have a greater chance of escape in the endosomal compartment than if they had been recycled. Finally, the properties of the ionizable cationic lipids employed here have been optimized to destabilize surrounding membranes by association with endogenous anionic lipids (such as phosphatidylserine, PS, or lyso-bis phosphatidic acid, LBPA)⁵ to form membrane-lytic nonlamellar structures.^{4,5} It is conceivable that some of the siRNA release occurs in the lysosomes as the low pH (pH 4.5–5) in the lysosome will convert essentially all of the LNP ionizable cationic lipid to its positively charged, membrane lytic form. However, recent studies have shown that siRNA release occurs within 10 minutes of endocytosis²² in endosomes that have characteristics of both early and late endosomes,⁶ and little if any release is observed in lysosomes.²²

The third area of interest concerns whether enhanced gene silencing potency observed *in vitro* in the presence of NP3.47 can be extended to *in vivo* situations. As noted elsewhere the gene silencing potency of LNP-siRNA systems for hepatocyte targets is extremely high, requiring doses of as little as 10 μ g/kg body weight to achieve 50% gene silencing;^{3,4} however, for other tissues dose levels of 1 mg/kg body weight or more are required,^{23–25} limiting clinical applications. The addition of agents such as NP3.47 to enhance potency would appear an attractive option, however the problems associated with the likely toxicities of

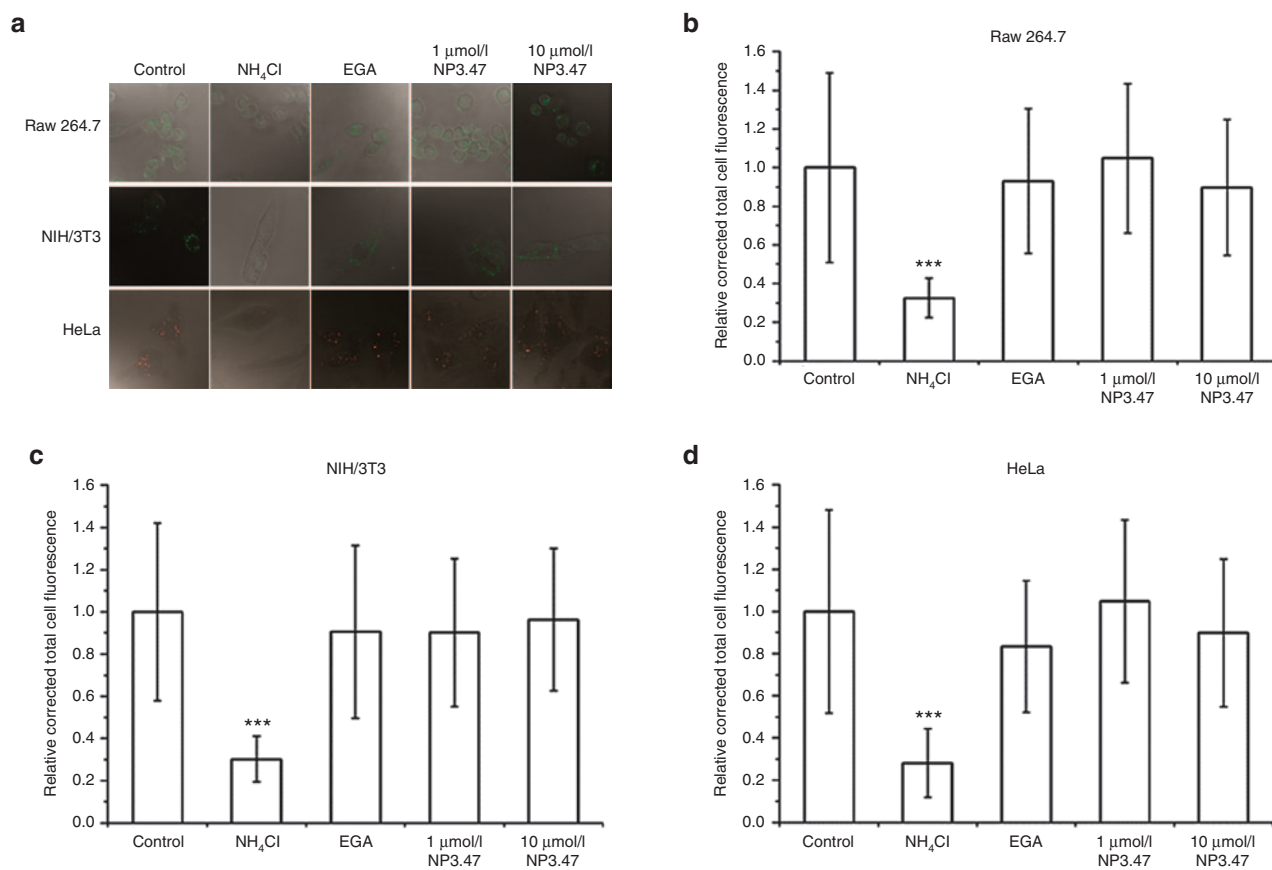


Figure 5 Acidic organelles are not neutralized by NP3.47. Cells were treated with compounds for 40 minutes at 37°C and stained with LysoTracker Green DND 26 (Raw 264.7 and NIH/3T3) or LysoView 633 (HeLa) to visualize acidic cell compartments. **(a)** Representative images of stained cells were imaged by confocal microscopy. Scale bar: 10 μm. Fluorescent intensities from confocal images of **(b)** Raw 264.7, **(c)** NIH/3T3, and **(d)** HeLa cells were quantified using ImageJ. On average at least 50 cells per experiment were analyzed. Quantification of fluorescent intensity per cell is expressed as corrected total cell fluorescence normalized to the untreated control cells. The data are presented as mean ± SD of three representative experiments performed in triplicate (***) $P < 0.001$ versus control by unpaired Student's *t*-test.

systemically administered NP3.47 limit the appeal of this option. In this regard we have recently shown²⁶ that a hydrophobic prodrug derivative of dexamethasone, when associated with LNP systems is a 20-fold or more potent for suppressing immunostimulatory effects of encapsulated RNA or DNA as compared with free dexamethasone. This is attributed to the avid accumulation of LNP systems by cells of the immune system such as macrophages and dendritic cells.²³ Thus, for specific tissues that avidly accumulate LNP systems, such as cells of the immune system, inclusion of a hydrophobic prodrug version of NP3.47 in the LNP may prove useful for increasing gene silencing potencies of LNP-siRNA systems.

In summary, the results presented here show that the NPC1 inhibitor NP3.47 leads to enhanced gene silencing capabilities for LNP-siRNA systems *in vitro*. The mechanism involved is consistent with inhibition of the NPC1 protein resulting in reduced LNP recycling to the cell exterior, greater accumulation of LNP-siRNA in intracellular organelles and concomitantly improved opportunities for escape of LNP-siRNA into the cell cytoplasm. It is anticipated that related strategies may be employed to enhance the potency of LNP-siRNA systems in certain tissues *in vivo*.

MATERIALS AND METHODS

Materials. The ionizable cationic lipid *O*-(*Z,Z,Z,Z*-heptatriacontan-6,9,26,26-tetraen-19-yl)-4-(*N,N*-dimethylamine) butanoate (MC3) was obtained from Biofine International (Vancouver, Canada). Polyethylene glycol-dimyristol glycerol (PEG-DMG) was synthesized as previously described by Akinc *et al.*,²⁷ 1,2-distearoyl-sn-glycero-3-phosphocholine (DSPC) and cholesterol were purchased from Avanti Polar Lipids (Alabaster, AL). Lipophilic dye DiI (1,1'-dioctadecyl-3,3,3'-tetramethylindocarbocyanine perchlorate) was obtained from Invitrogen (Carlsbad, CA). GAPDH siRNA (sense strand 5'-UGG CCA AGG UCA UCC AUG ACA ACU U-3' and antisense strand 5'-AAG UUG UCA UGG AUG ACC UUG GCC A-3') was purchased from Invitrogen. Filipin complex (F9765) and U 18666A were purchased from Sigma-Aldrich (St. Louis, MO). NPC1 inhibitor NP3.47 was synthesized following the procedures detailed elsewhere.⁹ The structure of NP3.47 was confirmed by NMR and the full details are provided in **Supplementary Method 1**.

Cell culture. The human cervix carcinoma cell line (HeLa), the murine macrophage cell line (Raw 264.7), the human prostate carcinoma cell line (PC3), and the murine fibroblast cell line (NIH/3T3) were cultured in Dulbecco's Modified Eagle's Medium (DMEM) containing 4 mmol/l L-glutamine, 4,500 mg/l glucose, 1 mmol/l sodium pyruvate, 1,500 mg/l sodium bicarbonate and supplemented with 10% (v/v) fetal bovine serum (FBS). The human prostate carcinoma cell lines (LNCaP and 22Rv1) and the human ovarian carcinoma cell line (OVCAR-3) were cultured in Roswell

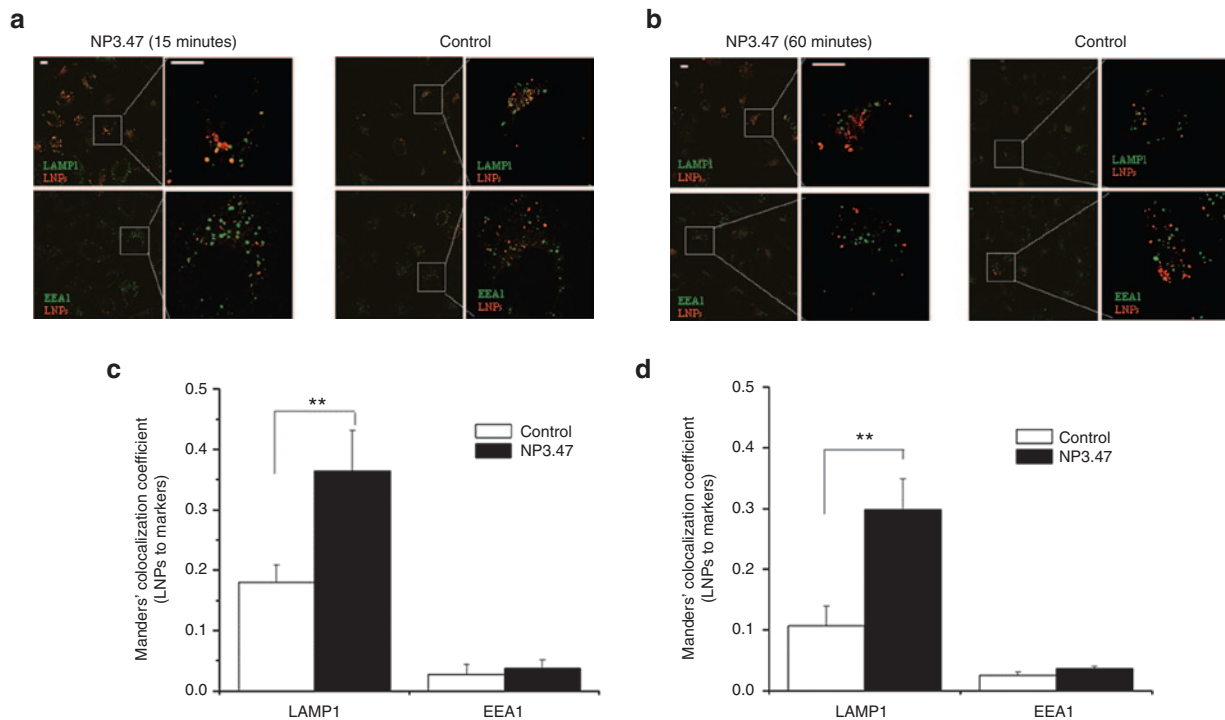


Figure 6 Treatment with NP3.47 results in increased localization of LNP-siRNA in late endosomal/lysosomal compartments. **(a, b)** Representative images of HeLa cells incubated with DiI-labeled LNP-siRNA (red) in the presence or absence of NP3.47 for 3 hours. Cells were fixed after 15 minutes **a** or 60 minutes **b** chase and stained with EEA1 or LAMP1 antibodies (green). The inset images show 282% magnification. Scale bar: 10 μ m. **(c, d)** Quantitative analysis of LNP colocalization with EEA1 and LAMP1 following 3 hours pulse and 15 minutes **c** or 60 minutes **d** chase. Data are presented as mean \pm SD based on three representative experiments, 8–10 images per experiment were analyzed (** $P < 0.01$ versus control by unpaired Student's *t*-test). EEA1, antiearly endosomal antigen-1; LAMP1, antilyosomal associated membrane protein-1; LNP-siRNA, siRNA-loaded LNP; LNP, lipid nanoparticle; siRNA, small interfering RNA.

Park Memorial Institute (RPMI)-1640 medium containing 2 mmol/l L-glutamine, 10 mmol/l *N*-2-hydroxyethylpiperazine-*N*-2-ethanesulfonic acid (HEPES), 1 mmol/l sodium pyruvate, 4,500 mg/l glucose, and 1,500 mg/l sodium bicarbonate and supplemented with 10% (v/v) FBS. The NPC1 knockout (NPC1^{-/-}) MEF cell line was a kind gift from G. Sahay at Oregon State University and P. Lobel at Rutgers University. NPC1^{-/-} cells were cultured in DMEM containing 10% FBS, 1% L-glutamate, 1% sodium pyruvate and 1% penicillin/streptomycin. All cell lines were kept in culture at 37°C in a humidified atmosphere containing 5% CO₂. All cell culture media and reagents were purchased from Invitrogen.

Preparation of siRNA LNPs. LNP-siRNA formulations were manufactured using a microfluidic mixing method as previously described.^{11,12} Briefly, MC3, DSPC, cholesterol, and PEG-DMG were dissolved in anhydrous ethanol at a molar ratio of 50:10:38.5:1.5 with a final lipid concentration of 20 mmol/l; A solution of siRNA at a final concentration of 0.28 mg/ml was prepared in 25 mmol/l sodium acetate buffer at pH 4. To formulate LNP-siRNA, lipid and siRNA solutions were injected into a microfluidic mixer (Precision Nanosystems, Vancouver, Canada) at flow rates of 1.5 ml/min (siRNA) and 0.5 ml/min (lipids) respectively, using two syringes controlled by a syringe pump (PHD Ultra, Harvard Apparatus, Holliston, MA). The LNP-siRNA preparations were then immediately dialyzed against a 50 mmol/l MES (BioShop, Burlington, Canada) and 50 mmol/l sodium citrate buffer (Sigma-Aldrich, Oakville, Canada) at pH 6.7 for at least 2 hours to remove residual ethanol, followed by dialysis against phosphate buffered saline (PBS) pH 7.4 overnight using 12–14 kD MWCO dialysis tubing (Spectrum Labs, Rancho Dominguez, CA). LNP-siRNA was subsequently passed through a 0.2 μ m filter (Pall, MI). The final cationic lipid/siRNA charge ratio was 3:1. LNP siRNA formulations were analyzed to determine siRNA encapsulation efficiency and LNP size. The LNP analysis is provided in **Supplementary Method 2** and **Supplementary Table S1**.

Intracellular accumulation of LNP-siRNA. HeLa, NIH/3T3, Raw 264.7, LNCaP, PC3, 22Rv1, OVCAR-3, or NPC1^{-/-} cells were seeded in black 96-well plates at a density of 6,000, 6,000, 10,000, 13,000, 6,000, 25,000, 10,000, and 6,000 cells per well, respectively. On the following day, cells were treated with DiI-labeled LNP-siGAPDH (0.5, 2.5, and 5 mg siRNA/l) and NP3.47 (0, 1 or 10 μ mol/l) and incubated for 24 hours. Cells were then fixed with 3% paraformaldehyde (PFA, Acros, NJ) containing 500 ng/ml Hoechst 33342 (Invitrogen) as a nuclear stain for 15 minutes at room temperature (RT). Cells were subsequently washed and stored in 100 μ l of PBS supplemented with 0.1 μ mol/l calcium chloride and 1 μ mol/l magnesium chloride. The plates were scanned with Cellomics ArrayScan VTI HCS Reader (Thermo Scientific, Pittsburgh, PA). Object identification and image analysis were performed using the Cellomics Compartmental Analysis algorithm. The average fluorescence intensity of DiI per well was measured.

Gene silencing. HeLa, PC3, 22RV1, OVCAR-3, or NPC1^{-/-} cells were seeded at a density of 100,000, 100,000, 250,000, 250,000, and 100,000 cells per ml in 24-well plate and grown overnight. LNP-siGAPDH at different concentrations (0.03, 0.1, and 0.3 mg/l) and 10 μ mol/l of NP3.47 or dimethylsulfoxide (DMSO) were added to the cells. After 24 hours, the cells were lysed and GAPDH mRNA level was quantified using RT-qPCR. Total RNA was isolated using PureLink RNA Mini Kits (Life Technologies, Carlsbad, CA) followed by cDNA synthesis using a High Capacity cDNA Reverse Transcription Kit (Applied Biosystems, Foster City, CA). Quantification of cDNA through RT-qPCR was performed using a TaqManFast Advanced Master Mix (Life Technologies), and PrimeTime Std RT-qPCR assay (GAPDH Hs.PT.58.40035104, and HPRT Hs.PT.58v.45621572; IDT, Coralville, IA). Data were analyzed and quantified using the Quantification Comparative C_T ($\Delta \Delta C_T$) analysis program of the StepOne Software Version 2.3 using the HPRT gene expression as an endogenous control.

Live cell imaging of the effects of small molecule inhibitors on acidic organelles. HeLa, NIH/3T3 or Raw 264.7 cells at a density of 100,000, 100,000 or 150,000 cells per ml, respectively, were seeded in 35-mm glass bottom culture dishes (MatTek, Ashland, MA). The following day, cells were treated for 40 minutes with 1 and 10 $\mu\text{mol/l}$ NP3.47, 5 $\mu\text{mol/l}$ EGA (ChemBridge, San Diego, CA), 25 mmol/l NH_4Cl or DMSO. Thereafter, HeLa cells were incubated with LysoView 633 (Biotium, Fremont, CA) for 15 minutes at 37°C while NIH/3T3 and Raw 264.7 cells were incubated with 75 nmol/l of LysoTracker Green (LTG) DND-26 (Life Technologies) in FluoroBrite DMEM (Life Technologies) for 2 minutes at 37°C. Cells were then washed with PBS and replenished with FluoroBrite DMEM (Life Technologies). Live cells were imaged immediately using a Leica confocal microscope (Leica, Wetzlar, Germany). LTG was excited using a 488 nm argon laser and imaged at 500–530 nm. LysoView 633 was excited with the 633 nm laser and imaged at 645–750 nm. LysoTracker and LysoView fluorescence intensity per cell was measured using ImageJ and expressed as corrected total cell fluorescence according to the method described by Potapova *et al.*,²⁸ The corrected total cell fluorescence was normalized to the untreated control cells.

Cellular recycling of LNP-siRNA. Cellular recycling of siRNA was determined according to Sahay *et al.*,⁷ Briefly, HeLa cells were seeded in 12-well plate at a density of 100,000 cells per ml and allowed to grow overnight. The following day, cells were treated with 1.5 mg/l of the fluorophore Quasar 570-labeled LNP-siRNA and 1 mg/l of ApoE (PeproTech, Rocky Hill, NJ), in the presence or absence of 10 $\mu\text{mol/l}$ NP3.47 for 3 hours. Cells were subsequently washed and incubated with fresh media containing 10 $\mu\text{mol/l}$ of NP3.47 or DMSO. At different time points (0, 2, 4, and 24 hours) the supernatants and cell lysates were collected. The fluorescence intensity of the cell lysates (intracellular) and the supernatant (extracellular) treated with and without 1% Triton X-100 was determined using Infinite M1000 microplate reader (Tecan, Männedorf, Switzerland). The siRNA concentrations at each time point were determined using a standard curve. At each time point, a ratio of extracellular siRNA concentration to the total siRNA concentration was plotted.

Intracellular localization of LNP-siRNA. HeLa cells were seeded and grown on glass cover slips in 12-well plates until 70% confluent. The cells were then incubated with 2 mg siRNA/L of DiI-labeled LNP-siRNA and 10 $\mu\text{mol/l}$ NP3.47 or DMSO for a 3 hours pulse. The pulse treatment was stopped by removing the media and washing the cells. Fresh media was added and the cells were chased for 15 and 60 minutes. At each time point, the cells were washed with PBS twice, fixed with 3% PFA for 15 minutes and permeabilized with 0.1% saponin (Sigma-Aldrich, Oakville, Canada) for 10 minutes. To visualize endosomal and lysosomal compartments, fixed cells were incubated with goat antiserum endosomal antigen-1 (EEA1, Santa Cruz Biotechnology, Dallas, TX, 1:250) and rabbit antilyosomal associated membrane protein-1 (LAMP1, Abcam, Cambridge, UK, 1:1,000) primary antibodies for 1 hour at RT. After washing, cells were incubated with donkey anti-goat IgG (H+L) Alexa Fluor 488 (1:500, Life Technologies) and goat anti-rabbit IgG (H+L) (1:500, Life Technologies) secondary antibodies. After washing, the cover slips were mounted on microscope glass slides containing SlowFade Gold antifade reagent (Invitrogen) and the mounting medium was air-dried for 2 hours or overnight before they were examined under a confocal microscope.

All Z-stack images were acquired using a Leica SP8 confocal microscope equipped with a 63 \times oil immersion lens and imaged at 488 nm (Alexa 488) and 561 nm (DiI). Quantification of DiI-labeled LNP-siRNA colocalization with endocytic markers was performed using the JACoP module in ImageJ. Colocalization analysis was performed using Manders colocalization coefficient.²⁹ In our experiments, the Manders colocalization coefficient was calculated using the whole image and expressed as the ratio of DiI-labeled LNP-siRNA in the EEA1 or LAMP1 labeled endocytic compartments.

Statistical analysis. Data was analyzed using OriginPro 8 software (OriginLab, Northampton, MA). Sample size, number of replicates, and statistical methods are listed in the figure legends for each experiment.

SUPPLEMENTARY MATERIAL

Figure S1. Cholesterol intracellular accumulation was observed in NP3.47 treated HeLa cells.

Figure S2. Treatment with NP3.47 results in increased localization of LNP-siRNA with lysosomal positive vesicles.

Table S1. Encapsulation efficiency and particle size of LNP-siRNA.

Supplementary Method 1. Structure confirmation of NP3.47.

Supplementary Method 2. Analysis of lipid nanoparticles.

ACKNOWLEDGMENTS

The authors thank Ying K Tam (Acuitas Therapeutics) for his helpful discussion, and Genc Basha (University of British Columbia) and Paulo J.C. Lin (Acuitas Therapeutics) for their assistance with confocal microscopy. The authors also acknowledge research funding from the Canadian Institutes for Health Research (CIHR, FRN11627), the Weston Brain Institute (RR130490), and MIRI grant from Brain Canada. R.v.d.M. is supported by funding from the European Union's Horizon 2020 research and innovation program under the Marie Skłodowska-Curie grant agreement No. 660426, and by a Veni STW grant (14385) from The Netherlands Organization for Scientific Research (NWO). The authors declare no conflict of interest. J.Z. and M.A.C. synthesized the compounds. S.C. did initial screening of the compounds and performed the part of gene silencing experiments. H.W. performed all other experiments and wrote the paper. R.v.d.M. and P.R.C. revised the manuscript. Y.Y.C.T. and P.R.C. provided supervision.

REFERENCES

- Wu, SY, Lopez-Berestein, G, Calin, GA and Sood, AK (2014). RNAi therapies: drugging the undruggable. *Sci Transl Med* **6**: 240ps7.
- Kanasty, R, Dorkin, JR, Vegas, A and Anderson, D (2013). Delivery materials for siRNA therapeutics. *Nat Mater* **12**: 967–977.
- Belliveau, NM, Huft, J, Lin, PJ, Chen, S, Leung, AK, Leaver, TJ *et al.* (2012). Microfluidic synthesis of highly potent limit-size lipid nanoparticles for *in vivo* delivery of siRNA. *Mol Ther Nucleic Acids* **1**: e37.
- Jayaraman, M, Ansell, SM, Mui, BL, Tam, YK, Chen, J, Du, X *et al.* (2012). Maximizing the potency of siRNA lipid nanoparticles for hepatic gene silencing *in vivo*. *Angew Chem Int Ed Engl* **51**: 8529–8533.
- Semple, SC, Akinc, A, Chen, J, Sandhu, AP, Mui, BL, Cho, CK *et al.* (2010). Rational design of cationic lipids for siRNA delivery. *Nat Biotechnol* **28**: 172–176.
- Gillieron, J, Querbes, W, Zeigerer, A, Borodovsky, A, Marsico, G, Schubert, U *et al.* (2013). Image-based analysis of lipid nanoparticle-mediated siRNA delivery, intracellular trafficking and endosomal escape. *Nat Biotechnol* **31**: 638–646.
- Sahay, G, Querbes, W, Alabi, C, Eltoukhy, A, Sarkar, S, Zurenko, C *et al.* (2013). Efficiency of siRNA delivery by lipid nanoparticles is limited by endocytic recycling. *Nat Biotechnol* **31**: 653–658.
- Platt, FM, Wassif, C, Colaco, A, Dardis, A, Lloyd-Evans, E, Bembli, B *et al.* (2014). Disorders of cholesterol metabolism and their unanticipated convergent mechanisms of disease. *Annu Rev Genomics Hum Genet* **15**: 173–194.
- Côté, M, Misasi, J, Ren, T, Bruchez, A, Lee, K, Filone, CM *et al.* (2011). Small molecule inhibitors reveal Niemann-Pick C1 is essential for Ebola virus infection. *Nature* **477**: 344–348.
- Lu, F, Liang, Q, Abi-Mosleh, L, Das, A, De Brabander, JK, Goldstein, JL *et al.* (2015). Identification of NPC1 as the target of U18666A, an inhibitor of lysosomal cholesterol export and Ebola infection. *Elife* **4**: e12177.
- Zhigaltsev, IV, Belliveau, N, Hafez, I, Leung, AK, Huft, J, Hansen, C *et al.* (2012). Bottom-up design and synthesis of limit size lipid nanoparticle systems with aqueous and triglyceride cores using millisecond microfluidic mixing. *Langmuir* **28**: 3633–3640.
- Chen, S, Tam, YY, Lin, PJ, Leung, AK, Tam, YK and Cullis, PR (2014). Development of lipid nanoparticle formulations of siRNA for hepatocyte gene silencing following subcutaneous administration. *J Control Release* **196**: 106–112.
- Broderick, KE, Chan, A, Lin, F, Shen, X, Kichae, G, Khan, AS *et al.* (2012). Optimized *in vivo* transfer of small interfering RNA targeting dermal tissue using *in vivo* surface electroporation. *Mol Ther Nucleic Acids* **1**: e11.
- Griffiths, G, Hoflack, B, Simons, K, Mellman, I and Kornfeld, S (1988). The mannose 6-phosphate receptor and the biogenesis of lysosomes. *Cell* **52**: 329–341.
- Ashfaq, UA, Javed, T, Rehman, S, Nawaz, Z and Riazuddin, S (2011). Lysosomotropic agents as HCV entry inhibitors. *Viral J* **8**: 163.
- Gillespie, EJ, Ho, CL, Balaji, K, Clemens, DL, Deng, G, Wang, YE *et al.* (2013). Selective inhibitor of endosomal trafficking pathways exploited by multiple toxins and viruses. *Proc Natl Acad Sci USA* **110**: E4904–E4912.
- Yoshimori, T, Yamamoto, A, Moriyama, Y, Futai, M and Tashiro, Y (1991). Bafilomycin A1, a specific inhibitor of vacuolar-type H(+)-ATPase, inhibits acidification and protein degradation in lysosomes of cultured cells. *J Biol Chem* **266**: 17707–17712.
- Goldman, SD and Krise, JP (2010). Niemann-Pick C1 functions independently of Niemann-Pick C2 in the initial stage of retrograde transport of membrane-impermeable lysosomal cargo. *J Biol Chem* **285**: 4983–4994.
- Luzio, JP, Pryor, PR and Bright, NA (2007). Lysosomes: fusion and function. *Nat Rev Mol Cell Biol* **8**: 622–632.

20. Akinc, A, Querbes, W, De, S, Qin, J, Frank-Kamenetsky, M, Jayaprakash, KN *et al.* (2010). Targeted delivery of RNAi therapeutics with endogenous and exogenous ligand-based mechanisms. *Mol Ther* **18**: 1357–1364.
21. Eltoukhy, AA, Sahay, G, Cunningham, JM and Anderson, DG (2014). Niemann-Pick C1 affects the gene delivery efficacy of degradable polymeric nanoparticles. *ACS Nano* **8**: 7905–7913.
22. Wittrup, A, Ai, A, Liu, X, Hamar, P, Trifonova, R, Charisse, K *et al.* (2015). Visualizing lipid-formulated siRNA release from endosomes and target gene knockdown. *Nat Biotechnol* **33**: 870–876.
23. Basha, G, Novobrantseva, TI, Rosin, N, Tam, YY, Hafez, IM, Wong, MK *et al.* (2011). Influence of cationic lipid composition on gene silencing properties of lipid nanoparticle formulations of siRNA in antigen-presenting cells. *Mol Ther* **19**: 2186–2200.
24. Lee, JB, Zhang, K, Tam, YY, Tam, YK, Belliveau, NM, Sung, VY *et al.* (2012). Lipid nanoparticle siRNA systems for silencing the androgen receptor in human prostate cancer *in vivo*. *Int J Cancer* **131**: E781–E790.
25. Di Paolo, D, Ambrogio, C, Pastorino, F, Brignole, C, Martinengo, C, Carosio, R *et al.* (2011). Selective therapeutic targeting of the anaplastic lymphoma kinase with liposomal siRNA induces apoptosis and inhibits angiogenesis in neuroblastoma. *Mol Ther* **19**: 2201–2212.
26. Chen, S, Zaifman, J, Tam, YY, Zhigaltsev, IV, Tama, YK, Ciufolini, MA *et al.* (2016). Lipophilic dexamethasone prodrugs are potent suppressors of lipid nanoparticle mediated immune stimulation. Submitted.
27. Akinc, A, Zumbuehl, A, Goldberg, M, Leshchiner, ES, Busini, V, Hossain, N *et al.* (2008). A combinatorial library of lipid-like materials for delivery of RNAi therapeutics. *Nat Biotechnol* **26**: 561–569.
28. Potapova, TA, Sivakumar, S, Flynn, JN, Li, R and Gorbosky, GJ (2011). Mitotic progression becomes irreversible in prometaphase and collapses when Wee1 and Cdc25 are inhibited. *Mol Biol Cell* **22**: 1191–1206.
29. Cordeliers, FP and Bolte, S (2008). In: *Proceedings of the 2nd ImageJ User and Developer Conference*. pp. 174–181.